

PSNR Based Optimization Applied To Maximum A Posteriori Expectation Maximization For Image Reconstruction On A Multi-Core System

¹A.Bharathi Lakshmi,

Assistant Professor & Head of IT, V.V.Vanniaperumal College For Women, (Autonomous), Virudhunagar, Tamil Nadu, India. bharathilakshmi@vvvcollege.org

²S.Kartheeswaran,

Assistant Professor, Department of Computer Science, Ayya Nadar Janaki Ammal College (Autonomous), Sivakasi, Tamilnadu, India. skarthiphd@gmail.com

³D.Christopher Durairaj,

Associate Professor, Research Centre in Computer Science, V.H.N.S.N College (Autonomous), Virudhunagar, kesterkaren@gmail.com

ABSTRACT

Statistical reconstruction methods present high potential image quality as compared to analytical methods; however, it suffers of time complexity. To reduce reconstruction time statistical reconstruction algorithm such as Maximum a Posteriori via Expectation Maximization algorithm (MAPEM) is parallelized in a shared memory processing (SMP) environment. This work exposes a parallel MAPEM algorithm that reconstructs an image on a multi-core parallel environment to reduce the execution time. An attempt to optimize the iteration required to reconstruct an image in various angle is performed. The execution time and speed up and efficiency factors for both serial and parallel MAPEM are computed. The present work uses phantom data sets of various sizes under different number projections. The research exhibits that the parallel computing environment provides the source of high computational power leading to reconstruct an image instantaneously.

Keywords—Image Processing, Image Reconstruction, Iterative Image Reconstruction, Statistical Iterative Methods, Likelihood Estimation, Maximum a Posteriori Expectation Maximization, Parallel Processing, OpenMP, Shared Memory Processor

I. INTRODUCTION

Image reconstruction Techniques (IRTs) is a mathematical process that produces images from the projection data obtained at various angles around an object with the help of some of the medical imaging modalities like Computed Tomography (CT), Magnetic Resonance (MR) or Positron Emission Tomography (PET). The reconstruction shows an energetic role in image processing method. It increases the quality of image, accuracy. Reconstruction is the method that is used to drop the radioactivity dosage. The medical image reconstruction follows the set of measurements of the image and performs the remote sensing mechanism. CT is a method that produces a tomographic image from the X-ray projection at different perspective near to the patient [1]. MRI scanner use the K space method to assemble the data, it reframes the images. The partial type of images contains low quality images. Image processor is used to remove the K space mistakes, it separates and forward the image to the reconstruction process. The reconstruction algorithm is applied on the partial images, it reduces the noise and reconstructs the images with high quality. The PET is an imaging technique that uses the tiny number of energetic compounds (tracker) to identify the disease. The active compounds are introduced into the body either injection or gas format. It displays the organs performance and presents a nervous system in detail. The tracker takes more time to scan the entire human body. The PET scanning process takes minimum of 30 to 60 minutes to finish the complete scan. The image reconstruction process takes place to avoid the blur images to obtain the clear images. X-Ray is a scan image that supports the reconstruction process with the help of CT image. The tomogram is a procedural term for a Computer Tomography image. It chooses the images in the form of slice, it corresponds to the what object being scanned, a CT slice represents to a specific thickness of the object being scanned. The voxels are used to compose the CT slice images.

Image reconstruction has been conceded using various reconstruction algorithms [1, 2]. Reconstruction methods utilize projection data as input and generate the estimate value that resembles the internal structure as output [3, 4]. Reconstruction methods utilize projection data as input and generate the estimate that resembles the internal structure as output [4, 5]. The projections are obtained using the detector ring around the object and are reconstructed using various

reconstruction algorithm [2]. Data sets with 36 projections measured from 0^0 to 180^0 around the phantom object were considered in the present study. The same dataset was used for testing the capability of the algorithms from a restricted number of projections, by skipping projections at uniform angular distribution. The research study presented here explores various reconstruction techniques using these types of projections.

Analytical and Iterative methods are classified as Image Reconstruction algorithms. The Analytical image reconstruction methods uses noise free images. Back Projection (BP) and Filtered Back Projection (FBP) reconstructs the image based on direct inversion of the radon transform derived using a continuous line integral. FBP introduces streak artifacts due to limited number of photon emission. Regardless of this disadvantage, FBP is expansively used in nuclear medicine because of its fast reconstruction time [2]. FBP reconstructs the image based on direct inversion of the radon transform derived using a continuous line integral. FBP introduces streak artifacts due to limited number of photon emission. Regardless of this disadvantage, FBP is expansively used in nuclear medicine because of its fast reconstruction time [6]. For noisy projection data as well as for a limited number of projections, the FBP method of image reconstruction shows very poor performance. Hence currently there is considerable interest to evaluate the use of other reconstruction methods for medical imaging techniques [5]. FBP algorithm produces high-quality images with excellent computational efficiency. However, FBP produces low Signal-to-Noise Ratio (SNR) images when a limited number of projections is used [7]. An Iterative method using a non-linear fit to the projection data has shown to give ripple free images [8]. Iterative Methods are based on optimization strategies incorporating specific constraints about the object and the reconstruction process. The iterative method can be classified into Algebraic and Statistical methods. Some of the accepted Algebraic iterative algorithms are Additive Algebraic Reconstruction Technique (AART) and Multiplicative Algebraic Techniques (MART) [7].

Statistical image reconstruction plays a vital role in the medical field. Statistical methods for image reconstruction can provide spatial resolution and noise properties over conventional Filtered Back Projection (FBP) methods [5]. However, such methods suffer from time complexity. The statistical method is considered as an iterative method in that it can be divided into weighted and likelihood [9]. As the repetition steps are high in the statistical method, it does not suit for all approaches. Iterative process includes the different methods for statistical reconstruction technique in the form of Poisson process. The Poisson statistical model supports the maximum posteriori work, maximum likelihood, context-based Bayesian framework. Expectation Maximization (EM) is one type of statistical method for image reconstruction process. EM Algorithm is an iterative algorithm that is often used for estimating parameters of Gaussian Mixture Model [10].

The present study has proven the time complexity reduction through speedup and efficiency by Amdahl's law. This work exposes a parallel MAPEM algorithm that reconstructs an image on a multi-core parallel environment to reduce the execution time. Parallel computing is emerging as a principal theory in high performance computing. Recently Shared Memory Processor(SMP) has been utilized for parallel computing. The SMP environment consists of a number of processors accessing one or more shared memory modules. For processing the large size of data, the SMP has some benefit over the distributed memory parallelization

II. METHODOLOGIES

This research helps for the projection of medical images like MEG, EEG, MRI, CT, and PET with the reduced time complexity. The image reconstruction using MAPEM will improve the resolution and reduce the noise of the images. MAPEM is introduced with a prior knowledge as a constraint that favours convergence of the expectation maximization algorithm process called as regularization. The prior is usually chosen to penalize the noisy images. The goal of the required criterion are simultaneously maximized which leads to a scheme called One Step Late (OSL) algorithm. The priori term is the derivative of an energy function chosen to enforce smoothing and a value is chosen to modulate the importance of the priori.

At the initial condition the reconstruction method guesses the estimate value that resembles the internal structure, by feeding projection data as input. This proposed work, develops MAPEM algorithm to reconstruct the image sequentially and works in Parallelized shared memory processing environment using different projection data sets. The experiment is carried out by the projection of Shepp logan phantom from Radon function available in MATLAB

Under the estimation theory the expectation maximization is a general optimization technique, to analyse the maximum likelihood estimation of parameters based on the tactical model. The E-Step, and the M-Step are the two steps involved in the EM algorithm. For every iteration in EM, the re-estimated parameters provides a least log likelihood value same as the previous values. The E-step, estimated parameter will calculate the maximum likelihood based on true value. In the M-step the calculated value in the E-step of maximum likelihood is used to estimate the parameters [11].

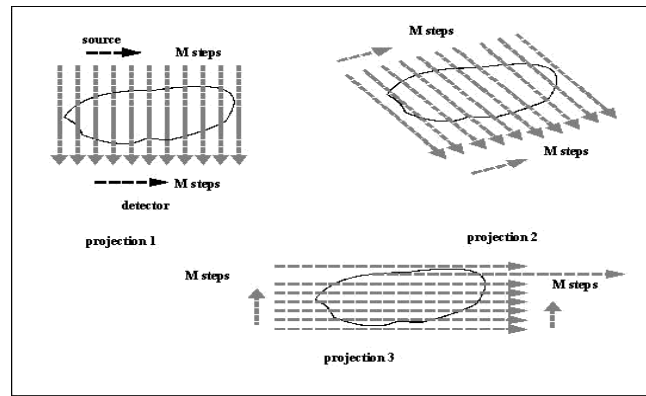


Figure 1: Three views of parallel beam projection of an EMI scanner

The parallel beam which determines a view or direction of the projection will be measured by an array consisting of a number of detectors, which will determine the number of sampling of the beam. Since the X-ray source can be assumed as point of the beam that pass a small fan shaped track can be assumed as a small beam itself. A small beam here is simply called as a ray. So a projection beam (view) consists of many projection rays (samplings). The three views of parallel beam projection of an EMI scanner have been presented in Figure 1.

The two steps will iterate continuously until the specified convergence is occurred. Applications of the EM algorithm include estimating class-conditional densities in supervised learning settings, density estimation in unsupervised clustering and for outlier detection purposes. The Spatial EM algorithm are based on the utilizes median based location and rank based scatter estimators to replace the sample mean and covariance matrix in the M – Step of an EM algorithm. Hence it improves the stability of the finite mixture model and it is well robust to outliers. There are also many good tutorials on EM algorithms. Thus the optimal solution, the maximum likelihood estimation directly leads to the accurate quantification as well as the reliability.



E-Step Procedure: Estimates the expectation of the missing value i.e. unlabelled class information. This step corresponds to performing classification of each unlabelled document. Probability distribution is calculated using current parameter.

The estimate is given from the previous iteration (m),

$$Q(\theta|\theta^{(m)}) = E_{x|y, \theta^{(m)}}[\log P(X|\theta)]$$

M-Step Procedure: Calculates the maximum likelihood parameters for the current estimate of the complete data.

$$\text{Maximize } Q(\theta|\theta^{(m)}) + \log P(\theta) \text{ Over } \theta \in \Theta$$

to find

$$\theta^{(m+1)} = \arg \max_{\theta \in \Theta} (Q(\theta|\theta^{(m)}) + \log P(\theta))$$

IRTs prove better in producing images of superior quality than the conventional filtered back projection-based algorithms. But in a clinical setting the use of IRT proves problematic because of the computational demands of these algorithms. Statistical methods for image reconstruction or restoration, such as Penalized Maximum-Likelihood (PML), Maximum Likelihood (ML), or Maximum A Posteriori (MAP), this methods have the challenge in the computation depends on the poisson log likelihood. Three different approaches are attempted aiming at shortening the computational time.

First the iterative reconstruction methods are applied with reduction in number of iterations. In second approach special hardware techniques were employed to do back projection on an event-by-event basis targeting at the speed of computations. Both these two approaches are not free from major problems. One significant problem was that computational speed arrived at was not remarkable but very limited. Moreover, it requires tremendous amount of computation. Hence the third approach that is parallel processing is considered promising and more reliable.

III. SYSTEM DESIGN AND IMPLEMENTATION

A. Data Set

In this research Shepp-Logan Phantom in various sizes 64 x 64, 128 x 128 and 256 x 256 is taken for study. The image data set is given in Figure 2. The Projections of the Shepp-Logan phantom are obtained using Radon function available in MATLAB at which angles the objects should be rotated. This system uses five different angles, such as 6° , 9° , 12° , 15° , 18° obtaining 30, 20, 15, 12, 10 numbers of projections respectively. The data read from the projections is supplied into the MEX function to execute under single and multiple processors.

Figure 2: The Shepp Logan Phantom Image of size (a)64x64 (b)128x128 (c) 256x256

B. Design and Implementation

- Sequential Version: The Figure 3 shows the flow diagram for the sequential MAPEM method. The flow shows that, in the initial condition it will read the projection data, apply E-step and M-step and update the vector. It then checks if error exists. If error exists, the process continues else the projection image will be displayed or else the process will be continued.

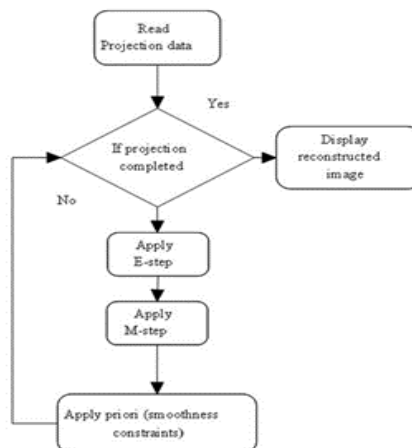


Figure 3: Flowchart showing the steps of MAPEM to reconstruct an image in sequential version

The EM technique is separated into two sections as E-step and M-step. The E-step, calculates the maximum likelihood based on true value. The M-step update the values using the value obtained from the E-step to estimate the parameters. Once the error value is not found it will be moved for the smoothness process for improving the resolution and to reduce the noise of the projection images. This operation will happen sequentially resulting in time complexity. The algorithm for the sequential version of MAPEM is given in Algorithm 1.

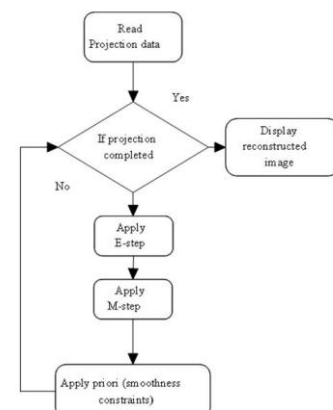
Algorithm 1 MAPEM Algorithm

Input: a, p, M, numIter

Output: retv

```

1: function mlem(a, p, M, numIter)
2:   retV ← zeros(numel(a), numIter)
3:   retV(:, 1) = a(:)
4:   nai2 ← full(sum(abs(M.* M), 2))
5:   I ← find(nai2 > 0)
6:   si ← size(I, 2)
7:   for j ← 1 to si do
8:     Mi ← full(M(j, :))
    
```



```

9:   norm  $\leftarrow$  norm +  $M_i'$ 
10:   end for
11:   for  $i \leftarrow 1$  to numIter do
12:     add_proj  $\leftarrow$  zeros(size(a))
13:     for  $j \leftarrow 1$  to  $s_i$  do
14:       if  $(j < \text{numel}(a) - 1) \ \&\& \ (j \neq 1) \ \&\&$ 
          $(M(j) \neq 1)$  then
15:          $K \leftarrow j - 1$ 
16:         while  $k \leq j$  do
17:            $s \leftarrow s + M(j, k) * (a(j) - a(k))$ 
18:            $k \leftarrow k + 2$ 
19:         end while
20:       end if
21:       add_proj  $\leftarrow$  add_proj +  $(M_i' * p(j))$ 
          $/(\text{sum}(M_i' * a))$ 
22:     end for
23:      $a \leftarrow a * \text{add\_proj} / (\text{norm} + s)$ 
24:     retV(:, i)  $\leftarrow$  a
25:   end for
26:   return retv
27: end function

```

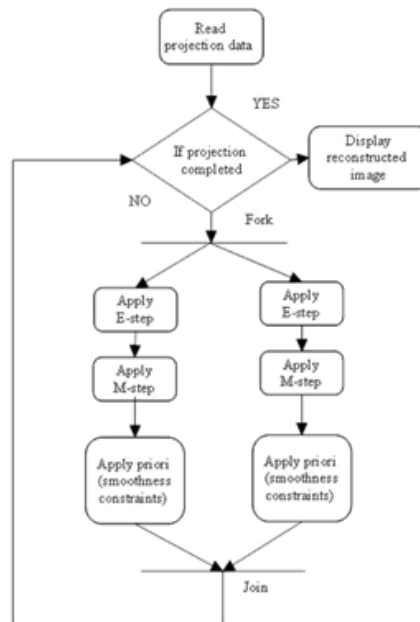


Figure 4: Flowchart of MAPEM to reconstruct an image in parallel mode

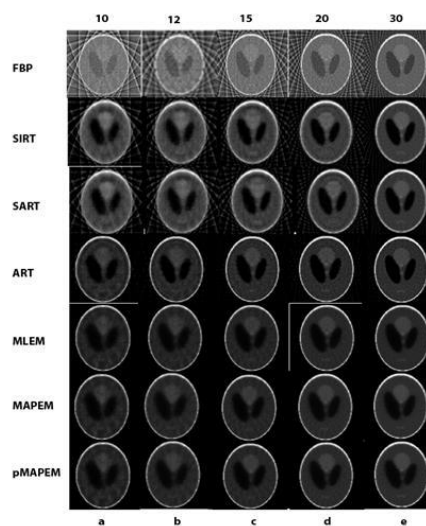
Parallel Version: The parallel version of MAPEM implemented on a multi-core environment is termed as parallel Maximum A Posteriori Expectation Maximization (pMAPEM). pMAPEM is same as the sequential operation, but with the help of OpenMP the operation will be functioned in multiple processes. For all the projection the E- step followed by the M-step will be carried out. In this method the operation will be done in parallel to reduce the time complexity. The master thread controls the worker thread by assigning the job to them. At the end the master thread collects all the values from worker thread and updates the value. The flowchart at Figure 3 illustrates the parallel version of pMAPEM. The parallel version Algorithm is given in Algorithm 2.

```

Input: a, p, M, numIter
Output: retv
1: function mlem(a, p, M, numIter)
2:   retV ← zeros(numel(a), numIter)
3:   retV(:, 1) = a(:)
4:   nai2 ← f ull(sum(abs(M.* M), 2))
5:   I ← f ind(nai2 > 0)
6:   si ← size(I, 2)
7:   omp_set_num_threads(numCore)
8:   n ← ceil(size(I, 1)/numCores)
9:   for j ← 1 to si do
10:    Mi ← f ull(M(j, :))
11:    norm ← norm + Mi'
12:  end for
13:  for i ← 1 to numIter do
14:    add_proj ← zeros(size(a))
15:    for j ← 1 to si do
16:      #pragma omp parallel for shared(si) private(j)
17:        schedule(dynamic, n) reduction(+ : v)
18:      if (j < numel(a) - 1) && (j 6= 1) && (M(j) 6= 1) then
19:        k ← j+1
20:        while k ≤ j do
21:          s ← s + M(j, k) * (a(j) - a(k))
22:          k ← k + 2
23:        end while
24:      end if
25:      add_proj ← add_proj + (Mi' * p(j))/(sum(Mi' * a))
26:    end for
27:    a ← a * add_proj/(norm + s)
28:    retV(:, i) ← a
29:  end for
30:  return retv
31: end function

```

IV. RESULTS AND DISCUSSION



In this research work statistical image reconstruction method MAPEM reconstruct a good quality image even in minimum number of projections compared to the Algebraic iterative methods. Figure 5 shows the GUI Designed and result obtained using MAPEM and pMAPEM.

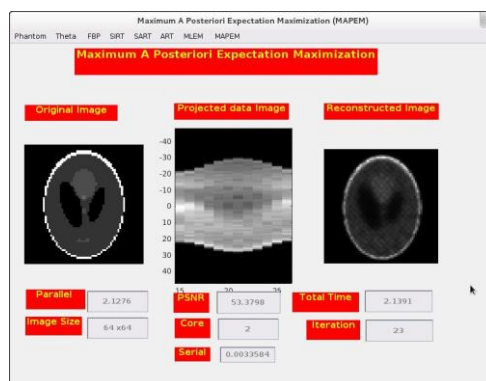


Figure 5: GUI of an MAPEM & pMAPEM

The parameters used to reconstruct an image size 64 x 64, 128 x 128 and 256 x 256 are projection matrix at angles 18° , 15° , 12° , 9° and 6° angles obtaining 10, 12, 15, 20 and 30 number of projections respectively, the weight vector as sparse matrix and optimized number of iterations based on the number of projections.

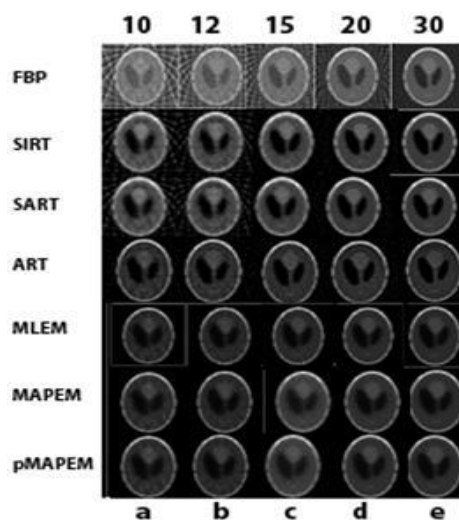
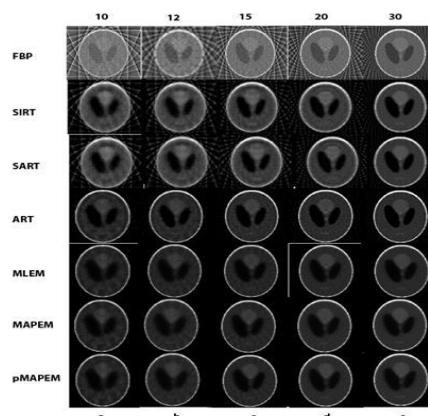


Figure 6: 64 x 64 image reconstructed using FBP, SIRT, SART, ART, MLEM, MAPEM and pMAPEM. Column represents the image reconstructed using the (a) data taken at 18° angles with 10 number of projections, (b) 15° angles with 12 number of projections, (c) 12° angles with 15 number of projections, (d) 9° angles with 20 number of projections, (e) 6° angles with 30 number of projections.

The images obtained for various sizes considered for study using the designed GUI application is given in the Figure 6, Figure 7 and Figure 8.



In all the figures the image reconstructed using FBP is at First row, SIRT is at second row, SART is at third row, ART is at fourth row, MLEM is at fifth row, MAPEM and pMAPEM is at sixth and seventh rows respectively. The column named (a), (b), (c), (d) and (e) denotes the image reconstructed using 10, 12, 15, 20 and 30 number of projections. SIRT, SART, ART, MLEM and MAPEM are executed sequentially where pMAPEM are implemented as parallel version. The last row in all the figures shows only pMAPEM that uses 2, 4 or 8 cores. The image reconstructed using any number of cores reconstructs same quality of image as MAPEM reconstruct in sequential version.

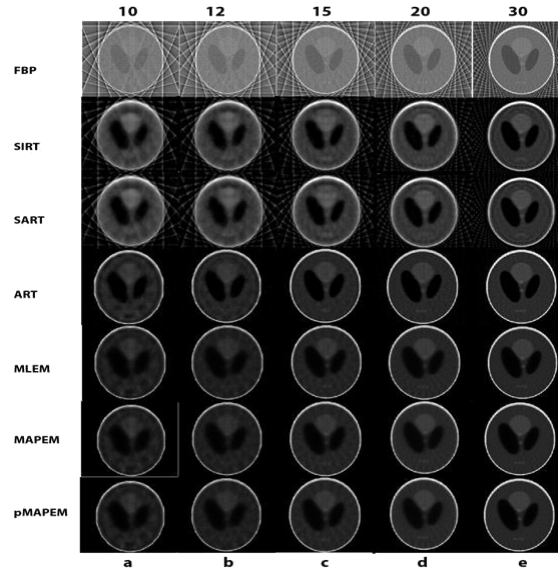


Figure 7: 128 x 128 image reconstructed using FBP, SIRT, SART, ART, MLEM, MAPEM and pMAPEM. Column represents the image reconstructed using the (a) data taken at 18° angles with 10 number of projections, (b) 15° angles with 12 number of projections, (c) 12° angles with 15 number of projections, (d) 9° angles with 20 number of projections, (e) 6° angles with 30 number of projections.

Figure 8: 256 x 256 image reconstructed using FBP, SIRT, SART, ART, MLEM, MAPEM and pMAPEM. Column represents the image reconstructed using the (a) data taken at 18° angles with 10 number of projections, (b) 15° angles with 12 number of projections, (c) 12° angles with 15 number of projections, (d) 9° angles with 20 number of projections, (e) 6° angles with 30 number of projections.

A. Iterations

The optimized number of iteration obtained using MAPEM image reconstruction algorithm is tabulated in the Table 1. The SIRT, SART algorithm uses the same iterations that have been optimized by the MAPEM algorithm.

TABLE I. OPTIMIZED ITERATION TO RECONSTRUCT 64 x 64, 128 x 128 256 x 256 IMAGE WITH HIGH PERCEPTUAL FIDELITY.

| Size | Iteration | | | | |
|-----------|-----------|----|----|----|----|
| | 10 | 12 | 15 | 20 | 30 |
| 64 x 64 | 19 | 23 | 10 | 18 | 20 |
| 128 x 128 | 41 | 23 | 35 | 27 | 27 |
| 256 x 256 | 61 | 39 | 45 | 29 | 61 |

From the Table 1 it is clear that as the image size increases the number of iterations gradually increases. Although number of projections increases the iterations remains the same for maximum number of projections as for the minimum number of projections.

B. Peak Signal-to-Noise Ratio

Table 2 is used to analyse the PSNR value for different image sizes with various number of projections. It is observed that the PSNR for different size of images using various angles is above 60 db which shows the tremendous perceptual fidelity.

TABLE II. MEASURED PSNR VALUES USING FBP, SIRT, SART, MAPEM AND pMAPEM ALGORITHMS WITH 10, 12, 15, 20 AND 30 NUMBER OF PROJECTIONS FOR VARIOUS IMAGE SIZES 64 x 64, 128 x 128 AND 256 x 256..

| Size | Algorithm | PSNR | | | | |
|-----------------|-----------|---------|---------|---------|---------|---------|
| | | 10 | 12 | 15 | 20 | 30 |
| 64 x 64 | FBP | 49.497 | 50.0059 | 50.7319 | 51.4147 | 51.9243 |
| | SIRT | 52.2959 | 52.5904 | 52.2921 | 53.0862 | 53.3409 |
| | SART | 52.3645 | 52.6329 | 52.5692 | 53.2317 | 53.4897 |
| | MAPEM | 53.5372 | 53.5798 | 53.5974 | 53.5882 | 53.3685 |
| | pMAPEM | 53.5372 | 53.5798 | 53.5974 | 53.5882 | 53.3685 |
| 128 x 128 | FBP | 49.497 | 54.6397 | 55.8001 | 57.0232 | 58.7456 |
| | SIRT | 59.0597 | 59.231 | 59.8758 | 60.306 | 60.9639 |
| | SART | 59.0982 | 59.2974 | 59.9331 | 60.4298 | 61.1544 |
| | MAPEM | 61.6712 | 61.233 | 62.1311 | 62.0966 | 62.1582 |
| | pMAPEM | 61.6712 | 61.233 | 62.1311 | 62.0966 | 62.1582 |
| 256 x 256 | FBP | 58.0899 | 59.0863 | 60.4143 | 62.0325 | 64.4252 |
| | SIRT | 65.3235 | 65.6486 | 66.345 | 66.9003 | 68.5452 |
| | SART | 65.351 | 65.6801 | 66.3955 | 67.0409 | 68.6266 |
| | MAPEM | 69.5812 | 69.7039 | 70.251 | 70.3148 | 71.0151 |
| | pMAPEM | 69.5812 | 69.7039 | 70.251 | 70.3148 | 71.0151 |

MAPEM shows better performance even for limited number of projections. The above result strongly reveals that statistical algorithm works fine even for small size images in minimum number of projections yielding a good PSNR value in a reasonable time. An attempt is made to reduce the time which can survey as a tool in medical field to reconstruct an image instantaneously.

C. Time Complexity

Time complexity is measured as the time taken by MAPEM for various image sizes to reconstruct in sequential and parallel using 1, 2, 4 and 8 cores in AMD processor. This time complexity of the reconstructed images with various size is given by the 2, 4, 8 cores in regard to the number of projections. Tables 3 tabulates the time complexity.

TABLE III. TIME TAKEN TO IMAGE OF VARIOUS SIZES WITH VARYING ALGORITHMS USING 10, 12, 15, 20 AND 30 NUMBER OF PROJECTIONS.

| Size | Algorithm | Time Taken | | | | |
|-----------------|---------------------|------------|----------|----------|----------|----------|
| | | 10 | 12 | 15 | 20 | 30 |
| 64 x 64 | FBP | 0.002 | 0.008099 | 0.006877 | 0.00332 | 0.011966 |
| | SIRT | 0.74811 | 0.62328 | 0.55388 | 1.385 | 1.9381 |
| | SART | 0.48602 | 0.6842 | 0.42174 | 1.0409 | 1.6463 |
| | MAPEM | 2.66441 | 3.79177 | 2.09434 | 5.26602 | 8.26126 |
| | pMAPEM (2 Cores) | 2.25607 | 3.20836 | 1.3518 | 3.20718 | 6.32703 |
| | pMAPEM (4 Cores) | 1.33296 | 2.15583 | 1.14649 | 3.01207 | 4.43421 |
| | pMAPEM (8 Cores) | 1.12781 | 1.57789 | 0.86358 | 2.00983 | 3.07759 |
| 128 x 128 | FBP | 0.005284 | 0.0037 | 0.004395 | 0.005571 | 0.009635 |
| | SIRT | 8.2162 | 4.5569 | 11.0323 | 8.057 | 18.671 |
| | SART | 6.9792 | 4.9261 | 8.5043 | 9.9196 | 13.096 |
| | MAPEM | 43.4195 | 29.3706 | 56.6291 | 54.7103 | 84.1047 |
| | pMAPEM (2 Cores) | 39.0638 | 23.9133 | 47.5634 | 48.2149 | 67.2989 |
| | pMAPEM | 26.928 | 18.3259 | 44.5746 | 36.3727 | 50.3595 |

| | | | | | | |
|-----------------|---------------------|----------|----------|---------|----------|----------|
| | (4 Cores) | | | | | |
| | pMAPEM (8 Cores) | 21.8957 | 11.1107 | 21.8165 | 22.1902 | 31.908 |
| 256 x 256 | FBP | 0.008455 | 0.007704 | 0.00781 | 0.015839 | 0.021083 |
| | SIRT | 75.6588 | 76.6664 | 91.628 | 56.3881 | 176.8353 |
| | SART | 50.5161 | 57.6855 | 56.3243 | 56.3881 | 202.067 |
| | MAPEM | 726.522 | 532.309 | 727.098 | 532.317 | 771.465 |
| | pMAPEM (2 Cores) | 502.087 | 332.341 | 502.65 | 332.347 | 463.192 |
| | pMAPEM (4 Cores) | 398.953 | 297.146 | 399.495 | 297.143 | 447.483 |
| | pMAPEM (8 Cores) | 198.488 | 145.926 | 199.045 | 145.934 | 259.513 |

A graph has been plotted for the values tabulated in Table 3 in the Figure 9, Figure 10 and Figure 11 for image sizes 64 x 64, 128 x 128 and 256 x 256 respectively.

Graph plotted shows that MAPEM algorithm takes maximum time to reconstruct the image in all considered sizes. The objects of applying MAPEM algorithm are to reduce the time consumption and to improve the quality of the reconstructed image. Quality of the image is already proved by measuring the PSNR value tabulated in Table 2. The time consuming objective is obtained by parallelizing the algorithm under 2, 4 and 8 cores. The graph shows that image is reconstructed in minimum number of seconds using MAPEM under 8 Cores.

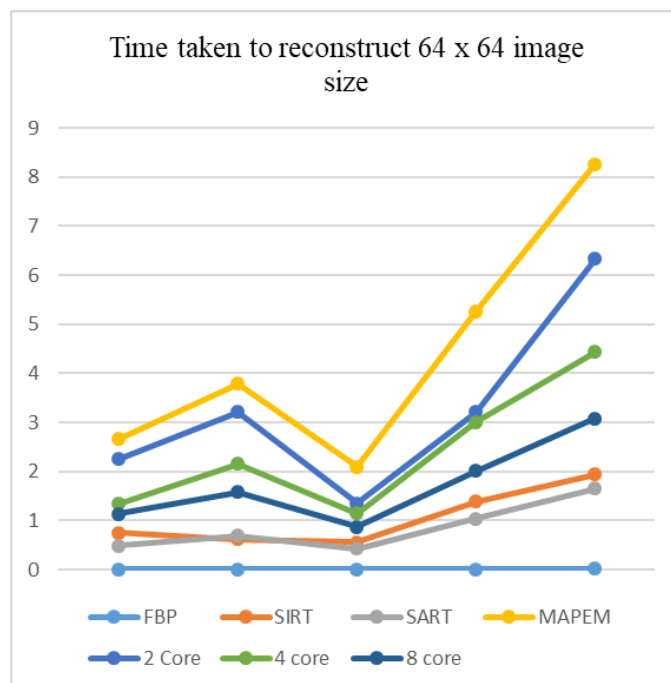


Figure 9: Time achieved to reconstruct 64 x 64 image with 10, 12, 15, 20 and 30 number of projections using FBP, SIRT, SART, MAPEM and pMAPEM using 2, 4 and 8 cores.

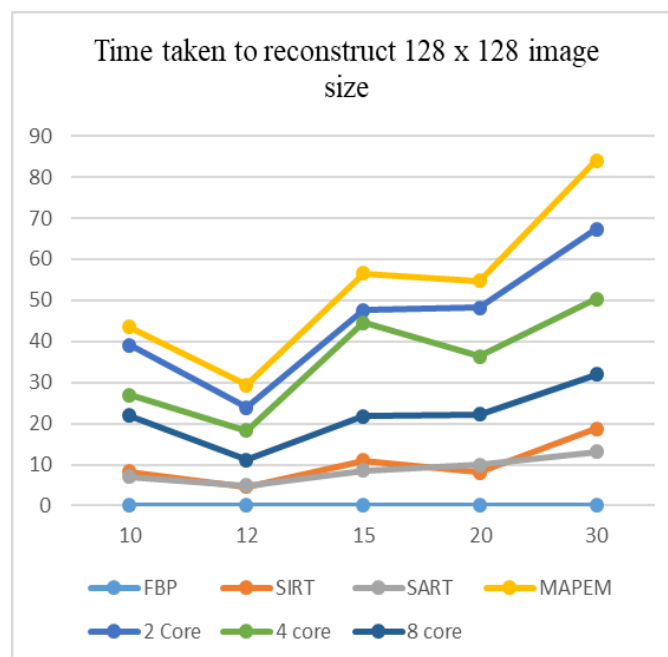


Figure 10: Time achieved to reconstruct 128 x 128 image with 10, 12, 15, 20 and 30 number of projections using FBP, SIRT, SART, MAPEM and pMAPEM using 2, 4 and 8 cores.

D. Speed Up

The performance analysis of a multi-core system can be estimated by the speedup factor of the number of processors used to execute. The speedup measures increase in running time due to parallelism. Speedup measures how much faster the computation executes versus the best serial code. The speedup is measured in ghz. The theory of speedup is established by Amdahl's law. The performance analysis measure is tabulated in Table 4.

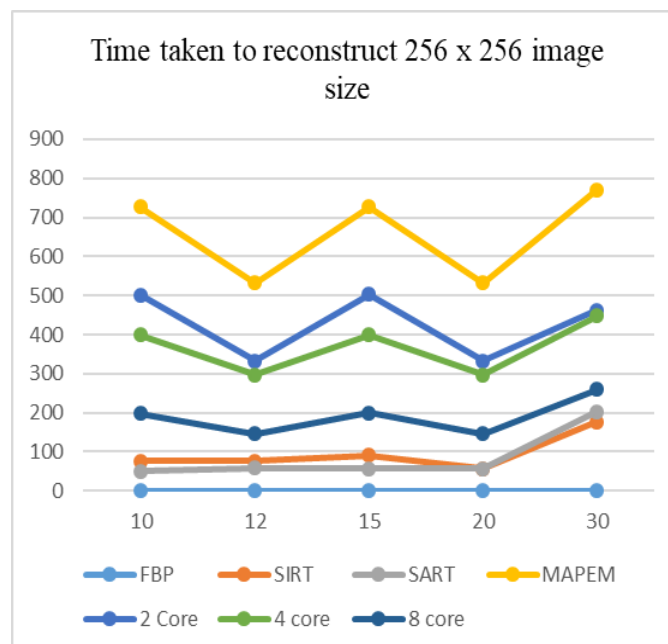


Figure 11: Time achieved to reconstruct 256 x 256 image with 10, 12, 15, 20 and 30 number of projections using FBP, SIRT, SART, MAPEM and pMAPEM using 2, 4 and 8 cores.

TABLE IV. TIME TAKEN TO IMAGE OF VARIOUS SIZES WITH VARYING ALGORITHMS USING 10, 12, 15, 20 AND 30 NUMBER OF PROJECTIONS.

| Size | Cores | 10 | 12 | 15 | 20 | 30 |
|-----------------|------------|---------|---------|---------|---------|---------|
| 64 x 64 | 1 Core | 1 | 1 | 1 | 1 | 1 |
| | 2 Cores | 1.47544 | 1.97114 | 1.98946 | 1.98291 | 1.97556 |
| | 4 Cores | 1.95798 | 3.80297 | 3.94194 | 3.88316 | 3.88814 |
| | 8 Cores | 2.30998 | 7.0474 | 7.69289 | 7.39583 | 7.16673 |
| 128 x 128 | 1 Core | 1 | 1 | 1 | 1 | 1 |
| | 2 Cores | 1.38349 | 1.97346 | 1.99118 | 1.97773 | 1.99661 |
| | 4 Cores | 1.73617 | 3.87638 | 3.95761 | 3.93252 | 3.93043 |
| | 8 Cores | 1.94444 | 7.62123 | 7.76133 | 7.58582 | 7.86187 |
| 256 x 256 | 1 Core | 1 | 1 | 1 | 1 | 1 |
| | 2 Cores | 1.27736 | 1.97445 | 1.99581 | 1.98687 | 1.99471 |
| | 4 Cores | 1.51692 | 3.91267 | 3.95574 | 3.8835 | 3.91221 |
| | 8 Cores | 1.6212 | 7.50019 | 7.74031 | 7.91742 | 7.71174 |

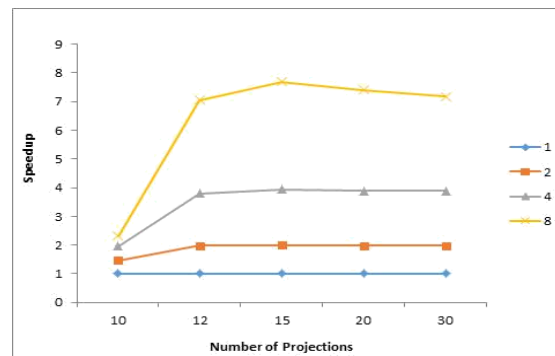


Figure 12: A graph showing the Performance Analysis of the multi-core environment for the image reconstructed for 64x64 at varying number of projections under 1, 2, 4 and 8 cores.

The Figure 12, Figure 13 and Figure 14 plots the speedup calculation against various projection angles considered for study and different number of cores 1, 2, 4 and 8 for different reconstructed image sizes.

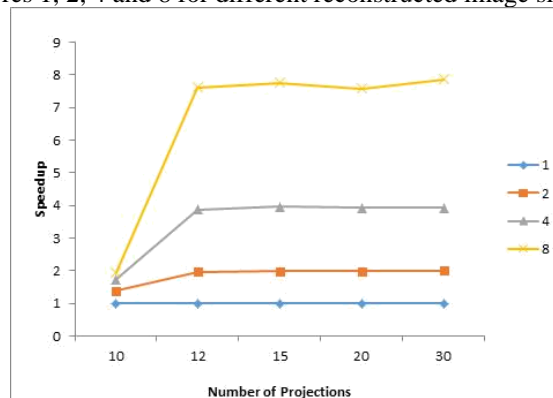


Figure 13: A graph showing the Performance Analysis of the multi-core environment for the image reconstructed for 128 x 128 at varying number of projections under 1, 2, 4 and 8 cores.

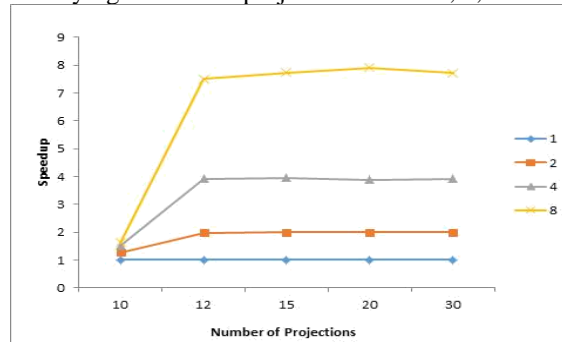


Figure 14: A graph showing the Performance Analysis of the multi-core environment for the image reconstructed for 256 x 256 at varying number of projections under 1, 2, 4 and 8 cores

All the graphs show that the performance gradually increases with increase in the number of cores. The speed up graph for all the sizes specified at different angles shows a good efficiency. This survey as the evidence of parallel programming applied at any field gives a better performance in reduction of time complexity.

V. SUMMARY

This paper deals with the Statistical reconstruction methods for high potential image quality as compared to analytical methods. However, it suffers from time complexity. In the proposed work the parallel MAPEM algorithm that reconstructs an image on a single as well as multi-core parallel environment is designed and implemented and proved that at multi core environment time complexity is reduced. The number of iteration mandatory to reconstruct an image is optimized. The images are reconstructed sequentially as well as in parallel environment using different projection data sets.

References

- [1] J. Treibig, G. Hager, H. G. Hofmann, J. Hornegger, and G. Wellein, "Pushing the limits for medical image reconstruction on recent standard multicore processors," *The International Journal of High Performance Computing Applications*, vol. 27, pp. 162-177, 2013.
- [2] R.Murugesan, M.Afeworki, J.A.Cook, N.Devasahayam, R.Tschudin, J.B.Mitchell, S.Subramanian, and M.C.Krishna. A broadband pulsed radio frequency electron paramagnetic resonance spectrometer for biological applications. *Review of Scientific Instruments*, 69(4), April 1998. (2)
- [3] G.L.Zeng. Image reconstruction a tutorial. *Computerized Medical Imaging and Graphics*, 25, 2001. (3)
- [4] P.Gilbert. Iterative Methods for the three dimensional reconstruction of an object from projections. *Journal of Theory, Biology*, 36, July 1972. (4)
- [5] P.M.V.Subbarao, P.Munshi, and K.Muralidhar. Performance of iterative tomographic algorithms applied to non destructive evaluation with limited data. *NDT and E International*, 30, 1997. (5)
- [6] J. Treibig, G. Hager, H. G. Hofmann, J. Hornegger, and G. Wellein, "Pushing the limits for medical image reconstruction on recent standard multicore processors," *The International Journal of High Performance Computing Applications*, vol. 27, pp. 162-177, 2013. (6)
- [7] S.Sivakumar, MuraliC.Krishna, R.Murugesan. Evaluation of Algebraic Iterative Algorithms for Reconstruction of Electron Magnetic Resonance Images, September 2010. (7)
- [8] C.N.Smith and A.D.Stevens. Reconstruction of images from radiofrequency electron paramagnetic resonance spectra. *The British Journal of Radiology*, 67, 1994. (8)
- [9] M. Beister, D. Kolditz, and W. A. Kalender, "Iterative reconstruction methods in X-ray CT," *Physica Medica: European Journal of Medical Physics*, vol. 28, pp. 94-108, 2012. (9)
- [10] G. Wang and J. Qi, "PET image reconstruction using kernel method," *IEEE transactions on medical imaging*, vol. 34, pp. 61-71, 2015. (10)
- [11] J. Ma, H. Zhang, Y. Gao, J. Huang, Z. Liang, Q. Feng, et al., "Iterative image reconstruction for cerebral perfusion CT using a pre-contrast scan induced edgepreserving prior," *Physics in Medicine & Biology*, vol. 57, p. 7519, 2012.